

Assimilation of EOS MLS ozone observations in the Met Office data-assimilation system

D. R. Jackson*
Met Office, Exeter, UK

ABSTRACT: In this paper the impact of Earth Observing System Microwave Limb Sounder (EOS MLS) observations on ozone analyses is investigated using the Met Office data-assimilation system. EOS MLS was launched in 2004, and produces high-quality ozone observations in the upper troposphere and stratosphere at high vertical and horizontal resolution. The experiments shown here are run using 3D-Var and a forecast model that has 50 levels – from the surface to approximately 63 km – and a horizontal resolution of 2.5° latitude by 3.75° longitude. Most of the experiments are run for the period January–February 2005.

The chief impact of assimilating EOS MLS data is a reduction of the mean analysis error, and of the standard deviation, in the lower stratosphere. Compared with control simulations, mean errors drop by 5%–25% in the Southern-Hemisphere extratropics, by around 10% in the Northern-Hemisphere extratropics, and by around 50% (with respect to ozonesondes) in the region of the tropical upper troposphere and lower stratosphere.

Further investigation shows that the improved ozone analyses in the Southern Hemisphere largely result from a much better representation of summertime low-ozone events. These events have been documented in the northern summer stratosphere, but never before in the southern summer stratosphere. In the Northern Hemisphere the addition of EOS MLS to the assimilation system is shown to lead to a better representation of winter polar ozone depletion. At low latitudes, it appears that errors in the background model transport fields often lead to errors in the ozone analysis, but that the addition of high-density, good-quality EOS MLS data alleviates much of this error. It is noted that the EOS MLS data have a more beneficial impact on ozone analyses in this region than do data from the Michelson Interferometer for Passive Atmospheric Sounding, which has a similar resolution and observational error to EOS MLS. © Crown Copyright 2007. Reproduced with the permission of Her Majesty's Stationery Office. Published by John Wiley & Sons, Ltd.

KEY WORDS ozone; data assimilation; stratosphere; EOS MLS

Received 30 March 2007; Revised 13 June 2007; Accepted 23 July 2007

1. Introduction

In recent years, ozone observations have been assimilated into a variety of different systems. These include general circulation models (GCMs), which incorporate simplified ozone chemistry (e.g. Jackson, 2004; Geer *et al.*, 2006a; Geer *et al.*, 2006b; Geer *et al.*, 2007; Dethof and Holm, 2004), and chemical transport models (CTMs), which incorporate detailed ozone chemistry but which are driven by off-line winds (e.g. Eskes *et al.*, 2003; Errera and Fonteyn, 2001). A variety of data-assimilation techniques have also been used to produce the ozone analyses. These include 3D-Var (e.g. Jackson, 2004; Geer *et al.*, 2006a; Geer *et al.*, 2006b; Geer *et al.*, 2007; Dethof and Holm, 2004), 4D-Var (e.g. Dethof, 2003; Errera and Fonteyn, 2001), the Kalman filter (e.g. Eskes *et al.*, 2003), and the physical-space statistical-analysis scheme (e.g. Stajner *et al.*, 2001). A benefit of the assimilation approach is that it can provide four-dimensional quality-controlled ozone analyses that make use of all ozone observations available to the assimilation system.

In addition, if the ozone is assimilated as part of a GCM system, there is the potential to improve analyses of other fields, such as temperature and wind. The primary reasons for this are:

- more accurate assimilation of satellite radiances from channels that are sensitive to ozone;
- utilization of correlations between ozone and wind to improve wind analyses in the upper troposphere and lower stratosphere (UTLS) (e.g. Riishojgaard, 1996); and
- more accurate radiative heating rates, and hence temperatures arising from using analysed ozone rather than climatological ozone in the forecast model radiation scheme (often referred to as 'ozone/radiation interaction').

In practice, it has been difficult to demonstrate these benefits: operational numerical weather-prediction (NWP) systems tend to use satellite data from channels that are not strongly sensitive to ozone; the difficulty of specifying error correlations between ozone and wind can lead to degraded rather than improved wind analyses (e.g. Holm *et al.*, 1999, 2000); and recent trials have

*Correspondence to: D. R. Jackson, Met Office, FitzRoy Road, Exeter EX1 3PB, UK. E-mail: david.jackson@metoffice.gov.uk

shown that the ozone/radiation interaction has little clear positive impact on temperature analyses and forecasts (e.g. Morcrette, 2003) – Cariolle and Morcrette (2006) state that in order to adequately represent the ozone radiative heating in the UTLS, ozone profiles with a vertical resolution of around 1 km need to be assimilated.

Furthermore, a potential by-product of a better representation of ozone in the NWP system is improved analyses and forecasts of surface ultraviolet (UV) radiation, but because the benefits listed above are hard to demonstrate, many operational NWP centres avoid the computational expense of adding ozone to their assimilation system, and the methods they use to provide surface UV forecasts often include a statistical, instead of an explicit, representation of ozone (e.g. Austin *et al.*, 1994).

Operational NWP systems, by their nature, must assimilate data that are available in near-real time. For ozone, these datasets include total-ozone observations from the Total Ozone Mapping Spectrometer (TOMS) and the Global Ozone Monitoring Experiment (GOME), partial ozone columns from the Solar Backscatter Ultraviolet Radiometer (SBUV), and satellite radiance measurements from ozone-sensitive channels such as the High-Resolution Infrared Sounder (HIRS) channel 9. These observations all have coarse vertical resolution, and thus the assimilation scheme has to rely on the ozone background-error covariances to distribute the observation–analysis increment in the vertical. This is difficult, and it frequently happens that the vertical distribution of the analysis increment is unrealistic and that the increment can smear out realistic vertical structure (e.g. Dethof and Holm, 2004).

Several ozone-assimilation studies have been carried out using ozone measurements from research satellites, which often have a better vertical resolution than the operational data mentioned above. For example, Struthers *et al.* (2002) assimilate data from the Upper Atmospheric Research Satellite (UARS) Microwave Limb Sounder (MLS), and Geer *et al.* (2006a) describe a series of assimilation experiments that use data from the Michelson Interferometer for Passive Atmospheric Sounding (MIPAS). In the latter study, an intercomparison is made of ozone analyses from many different analysis systems (CTM and GCM; 3D-Var, 4D-Var and Kalman-filter data assimilation; comprehensive, simplified and absent ozone chemistry). They find that in areas where MIPAS data quality is good, similar results are found irrespective of the ozone-assimilation system used. However, larger differences are seen in regions where MIPAS data are of low quality or where uncertainties in the modelling of ozone are higher, such as the troposphere, the tropical tropopause, the ozone hole, and the upper stratosphere and mesosphere.

In this paper, we assimilate ozone data from the Earth Observing System (EOS) Microwave Limb Sounder (MLS). This instrument is mounted on the EOS Aura satellite, which was launched on 15 July 2004. It provides observations between the upper troposphere and the lower mesosphere, with a vertical resolution of 3–4 km

(in the stratosphere) and comparatively high horizontal resolution (165 km along the suborbital track). The Aura satellite flies in a polar orbit, and orbits the Earth about 14 times per day. The aim of this study is to use the Met Office data-assimilation system to identify the improvements to ozone analyses that result from adding EOS MLS ozone data to the assimilation system. The results are potentially of great interest to operational NWP centres, for two reasons:

- if a clear positive impact to ozone analyses from EOS MLS data is shown, then there may be more chance of realizing the above-listed positive impacts of ozone analyses on other assimilated fields (for example, via the ozone/radiation interaction);
- although the EOS MLS data are generally not available in near-real time, any benefits from assimilating these data could very well also accrue from assimilating data from the next generation of satellite instruments, such as GOME II and the Infrared Atmospheric Sounding Interferometer (IASI), which fly on the recently-launched Metop satellite and which will be available in near-real time to operational centres.

The structure of this paper is as follows. The EOS MLS ozone data are described in Section 2, together with other observational data that are used to evaluate the observational analyses. The Met Office data-assimilation system is described in Section 3. The experimental results are presented in Section 4: first, the ozone analysis errors are summarized; then the ability of the assimilation system to represent low-ozone events (LOEs) in the southern polar stratosphere, Northern-Hemisphere polar ozone depletion, and ozone in the tropical UTLS is examined in more detail. Conclusions are given in Section 5.

2. Ozone datasets used

2.1. Assimilated data

In the data-assimilation experiments described in this paper, ozone data from both EOS MLS and SBUV instruments are assimilated. Details of these datasets are given below.

2.1.1. EOS MLS

The EOS MLS ozone profiles assimilated here are version 1.51 (for the January–February 2005 and January 2006 experiments) and version 1.52 (for the June 2006 experiment). There is no difference in the ozone profiles between the two versions. EOS MLS is on the NASA Aura satellite, which flies in a near-polar sun-synchronous orbit. There are around 14 orbits per day; on each orbit EOS MLS observations span a region from 82°S to 82°N; retrievals are made every 165 km along the suborbital track (Waters *et al.*, 2006). The vertical resolution of the profiles is around 3 km in the UTLS, degrading to around 4 km at 215 hPa and 6 km in the mesosphere. An initial assessment of these profiles has

been carried out by Livesey *et al.* (2005) and Froidevaux *et al.* (2006). The profiles are considered to be useful in the 215–0.46 hPa range. The retrievals have an overall accuracy of around 1% in the stratosphere, and typically less than 10% in the upper troposphere (although sometimes the accuracy is 30%–40% in the 200–300 hPa range). Comparison with other satellite data shows that in the stratosphere agreement is generally within 5%–10% with data from the Halogen Occultation Experiment (HALOE), the Stratospheric Aerosol and Gas Experiment (SAGE II), the Polar Ozone and Aerosol Measurement (POAM III) and the Atmospheric Chemistry Explorer (ACE). The bias with respect to these datasets tends to be slightly positive in the lower stratosphere and slightly negative in the upper stratosphere. There is also overall good agreement with balloon-borne ozone measurements made at Fort Sumner, USA. At 215 hPa, limited comparison with Southern-Hemisphere Additional Ozonesondes (SHADOZ) indicates that EOS MLS has a positive bias (sometimes up to 100%) in the Tropics.

Version 1.52 retrievals have recently been superseded by version 2.2 retrievals. The version 2.2 ozone retrievals are typically in better agreement with correlative measurements; and in particular the error in the vertical gradient of stratospheric ozone (which leads to positive biases in the lower stratosphere and negative biases in the upper stratosphere) is reduced (e.g. Froidevaux *et al.*, 2007; Jiang *et al.*, 2007; Livesey *et al.*, 2007).

2.1.2. SBUV

SBUV/2 is a nadir-viewing instrument that infers the ozone vertical profile by measuring sunlight scattered from the atmosphere in the middle ultraviolet. The retrievals are provided in 12 layers, but are combined at the European Centre for Medium-Range Weather Forecasts (ECMWF) into 6 layers in order to reduce observation correlations. The 6 layers are: 0.1–1 hPa, 1–2 hPa, 2–4 hPa, 4–8 hPa, 8–16 hPa, and from 16 hPa to the surface. The horizontal resolution is approximately 200 km. Contributions to the total error include calibration errors (due to instrumental drift), which range from 2% at 100 hPa to 5% at 0.5 hPa, and biases due to the solar zenith angle. A change in zenith angle from 30° to 60° can lead to systematic errors of between –1% and 1%, dependent on the channel. A comparison with SAGE data shows total r.m.s. errors of 5%–15% in the 100–0.3 hPa range (Bhartia *et al.*, 1995; Bhartia *et al.*, 1996).

2.2. Independent data for comparison

In Section 4, the assimilation results are evaluated by comparison with independent data from ozonesondes, HALOE and TOMS. These are described below.

2.2.1. Ozonesondes

Ozonesonde profiles have been obtained from the World Ozone and Ultraviolet Radiation Data Centre (WOUDC <http://www.woudc.org>). Most sondes are of the electrochemical-concentration-cell (ECC) type, but some are carbon-iodide or Brewer–Mast sondes. The total error for the ECC sondes is estimated to be between –7% and 17% in the upper troposphere, $\pm 5\%$ in the lower stratosphere up to 10 hPa, and between –14% and 6% at 4 hPa (Komhyr *et al.*, 1995). Errors are higher in the presence of steep ozone gradients and where ozone amounts are low. Furthermore, a laboratory comparison of the three sonde types (Smit *et al.*, 1998) shows that the precision of the non-ECC sondes is about $\pm 10\%$ – 15% , compared to $\pm 5\%$ for the ECC sondes. The precision is best for all sondes in the middle stratosphere, where ozone is maximal. The results of short-term ozonesonde intercomparison campaigns (e.g. Beekmann *et al.*, 1994; Kerr *et al.*, 1994; Smit *et al.*, 1998) indicate that in the lower stratosphere (12–27 km) the systematic difference between sonde types is less than 5%, and the random variability from one sonde to another is less than 5% for all sonde types.

2.2.2. HALOE

Version 19 HALOE retrievals are used here. The combined systematic and random uncertainty of single ozone profiles is between 9% and 25% in the lower stratosphere and between 9% and 20% in the upper stratosphere. The agreement with correlative measurements is typically better than 10% down to 200 hPa in the extratropics and down to 100 hPa in the tropics and subtropics (Bruhl *et al.*, 1996; Bhatt *et al.*, 1999). HALOE data are available for the period from 11 October 1991 to 21 November 2005.

2.2.3. TOMS

TOMS measures back-scattered ultraviolet radiances with high horizontal resolution (38 km by 38 km) and daily near-global coverage. Version 8 of the Level-3 total-ozone-column product is used here. This has partial corrections for calibration problems in the post-2000 TOMS data from the Earth Probe satellite, and improved retrievals under extreme conditions compared with version 7. A full validation of TOMS version 8 has not yet been published, but version-7 uncertainties have been estimated as about 2% for the random errors, 3% for the absolute errors, and somewhat more at high latitudes because of the higher zenith angle (McPeters *et al.*, 1998).

3. The Met Office assimilation system

The Met Office NWP system has recently been extended to allow the assimilation of ozone (Jackson and Saunders, 2002; Jackson, 2004; Geer *et al.*, 2006a; Geer *et al.*, 2006b; Geer *et al.*, 2007), but ozone is not

assimilated operationally. Here, EOS MLS ozone profiles and SBUV ozone densities are assimilated, together with all operational dynamical observations, using a stratosphere–troposphere version of the Met Office assimilation system. The assimilating forecast model has a horizontal resolution of 3.75° longitude by 2.5° latitude, and 50 levels in the vertical, from the surface to around 0.1 hPa. The model dynamical equations, including the transport scheme, have a semi-Lagrangian formulation (Davies *et al.*, 2005). The data assimilation uses 3D-Var (Lorenc *et al.*, 2000) with a time window of 6 h centred at the analysis time. Therefore, the greatest time error for an assimilated observation will be 3 h. Ozone is assimilated in a univariate manner, and no ozone/radiation interaction is included. Background-error covariances are uniform for all latitudes and longitudes, and are based on vertical covariance data supplied by ECMWF.

The system is otherwise as described in (Geer *et al.*, 2006a), except that no MIPAS data are assimilated, and the error in the ozone photochemistry parametrization scheme (Cariolle and Deque, 1986) has been fixed. Details of the impact of this correction appear in (Geer *et al.*, 2007). In addition, there is no parametrization of ozone destruction due to heterogeneous chemistry.

The assimilation code for the EOS MLS profiles is based on that used to assimilate retrieved profiles from MIPAS. The observation error is taken directly from the precision estimate supplied by the EOS MLS Science Team, and no bias correction related to the biases reported above is carried out.

The SBUV data are subjected to a quality-control procedure prior to use in the assimilation system, and observations with a solar zenith angle greater than 84° or with a quality flag greater than 0 are blacklisted. This blacklisting procedure follows what is done operationally at ECMWF (e.g. Dethof, 2003).

The initial conditions for the assimilation experiments are as follows. For the January–February 2005 and January 2006 experiments, the mass and wind fields are taken from the daily stratospheric analyses that were produced operationally by the Met Office until March 2006 (e.g. Swinbank *et al.*, 2004). For the June 2006 experiment, these fields are taken from the operational Met Office troposphere–stratosphere analysis, reconfigured from its original resolution of 0.375° latitude by 0.5625° longitude to a resolution of 2.5° latitude by 3.75° longitude. In all experiments, the ozone initial conditions are taken from the monthly-mean zonal-mean climatology of (Li and Shine, 1995).

4. Results

In this section, results from three assimilation trials are described. In the first trial (CTRL), background ozone is calculated by the forecast model but no ozone data are assimilated; in the second (SBUV), ozone data from SBUV are assimilated; and in the third (MLS), SBUV and EOS MLS ozone data are assimilated. The assimilation trials

are run for a month, from 26 January 2005 to 25 February 2005.

In Section 4.1, an initial comparison of the three runs is made via inspection of analysed zonal-mean ozone fields and of ozone analysis errors with respect to ozonesonde, HALOE and EOS MLS data. Then a more detailed investigation is made of regions where there are particularly striking differences between the assimilations made with and without EOS MLS data. These regions are the summer polar stratosphere (Section 4.2), the winter polar stratosphere (Section 4.3), and the tropical UTLS (Section 4.4).

The three-way comparison of the runs CTRL, SBUV and MLS is restricted to one month because of the computational expense involved in running these trials. However, MLS has been run for two other periods: January 2006 and June 2006. In Section 4.5, results from these periods are summarized, in order to ascertain whether the conclusions from the January–February 2005 trials are robust.

4.1. Ozone analysis errors

Figure 1 shows the monthly-mean zonal-mean ozone fields from the three analyses. All analyses make a reasonable job of reproducing the broad structure of the observed ozone field (e.g. Grooss and Russell, 2005), such as the ozone maximum near 30 km in the Tropics, and the ozonepause, whose structure follows that of the tropopause.

The differences between runs CTRL and SBUV show that ozone is reduced in the lower stratosphere when SBUV is assimilated. This may indicate that the ozone values in the initial conditions are too high and that the SBUV data are doing a reasonable job of correcting this bias. This is confirmed by Figures 2 and 3, which show analysis errors compared to ozonesondes and HALOE, respectively. Mean errors for SBUV are similar to or smaller than those for CTRL in most parts of the lower stratosphere. Exceptions are in the Northern Hemisphere near 100 hPa (for both ozonesondes and HALOE) and in the Tropics between around 30 hPa and 10 hPa (for HALOE only). Figures 2 and 3 show that the standard deviations of the errors for SBUV are similar to or slightly smaller than those for CTRL. This shows the marginal positive benefit to the analyses from assimilation of SBUV data.

Figure 1 shows that analysed ozone amounts in the mid- and high-latitude stratosphere drop even further when EOS MLS data are assimilated. Figures 2 and 3 show that at levels up to around 35 km (or 5 hPa) the overestimation of ozone at southern latitudes is considerably smaller in MLS than in the other two runs. The standard deviation of the errors is clearly smaller when compared to HALOE, and smaller at many levels when compared to ozonesondes. These results indicate that there is a mechanism for ozone loss that is not represented in CTRL (and therefore, since no ozone is assimilated in CTRL, not represented in the forecast model). A possible mechanism is chemical loss over the

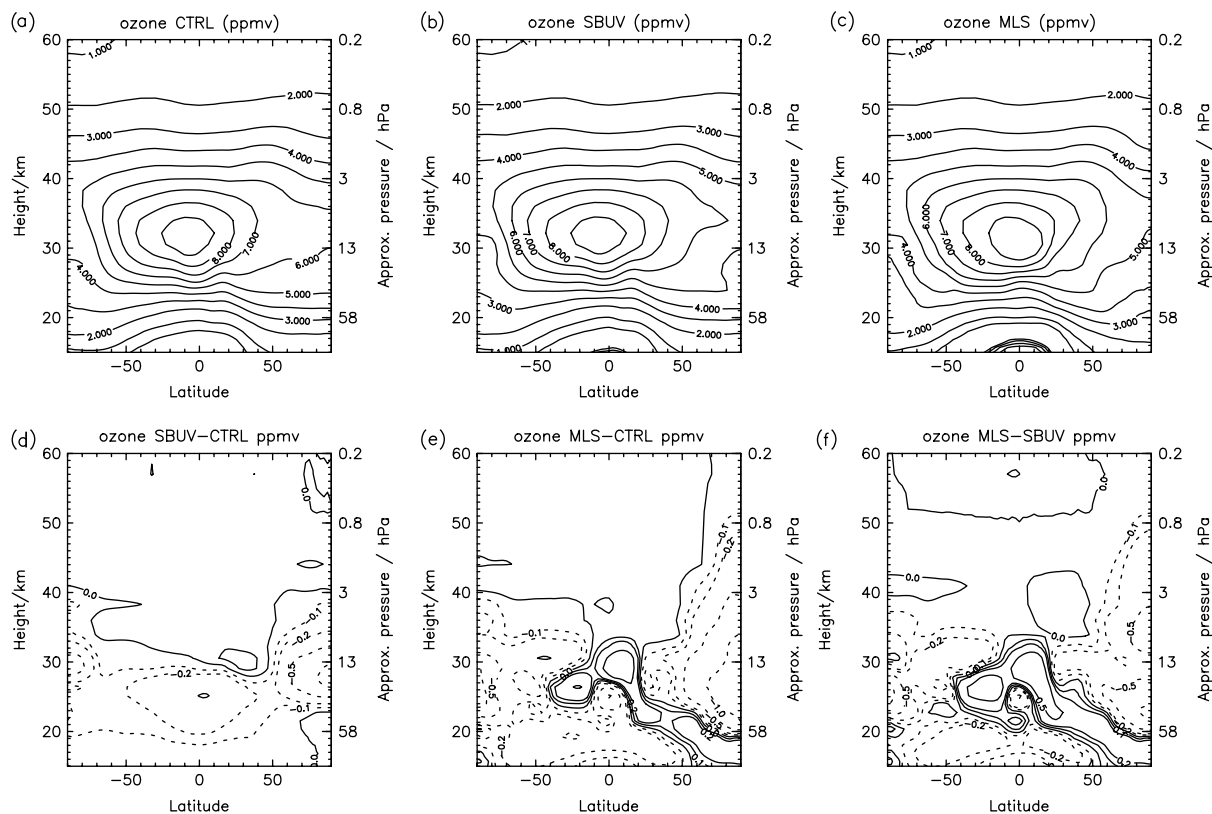


Figure 1. Zonal-mean ozone averaged over the period 1–25 February 2005: (a) run CTRL; (b) run SBUV; (c) run MLS; (d) difference between runs SBUV and CTRL; (e) difference between runs MLS and CTRL; (f) difference between runs MLS and SBUV.

summer pole during periods of very long days (Orsolini *et al.*, 2003; Orsolini and Nikulin, 2006), which gives rise to LOEs at high summer latitudes. The papers just cited document LOEs in the northern summer; the present paper is the first to report them in the southern summer stratosphere. The simulation of these LOEs is discussed further in Section 4.2.

Moving on to the Northern Hemisphere, Figure 1 shows that zonal-mean ozone values at northern polar latitudes are lower for SBUV and MLS than for CTRL. This could be attributed to ozone loss by heterogeneous chemistry, which is not represented in CTRL but is included, via the information from the SBUV and EOS MLS observations, in the other two runs. The 2004–2005 winter was the coldest on record (e.g. Manney *et al.*, 2006), and lower-stratospheric air during the experimental period was cold enough for polar stratospheric clouds (PSCs) to form. Figures 2 and 3 indicate that this loss is best represented in MLS, since the error standard deviation for this run is smaller than for the other two runs throughout the stratosphere. The mean error for MLS is also smallest in large parts of the stratosphere: below the 30 hPa level when compared to ozonesondes and between 30 hPa and 5 hPa when compared to HALOE. The difference in these results below the 30 hPa level is partly explained by the different spatial sampling of the HALOE and ozonesonde data used to calculate the mean errors. There are no HALOE data available north of 60°N during the analysis period, but several ozonesonde ascents are available at

these locations. Thus, the impact of large differences between MLS and the other runs at these latitudes (see Figure 1) will be captured by the errors calculated with respect to ozonesondes, but not with respect to HALOE. Figure 1 shows that at lower levels the vertical gradient of ozone across the tropopause is stronger in MLS than in CTRL and SBUV. Error standard deviations and mean error (compared to ozonesondes) in the UTLS are smallest for MLS, again indicating that the addition of MLS data improves the quality of the assimilation in the northern mid-latitude UTLS.

Figure 1 also shows that the vertical gradient of ozone near the tropopause is much stronger in MLS than in CTRL and SBUV. The latter two runs may have a weak gradient due to a combination of poor transport in the background field (Geer *et al.*, 2006a, section 5.6) and the low resolution of the SBUV data at these levels. It appears that the higher-resolution EOS MLS data, on the other hand, can resolve the ozone-field structure better. As a result, at low latitudes, ozone in this run is 0.1–0.2 ppmv lower than in the other two runs. Figure 2 shows that in the Tropics the ozone in CTRL and SBUV is considerably overestimated, particularly near the tropical tropopause (around 100 hPa) where the analysed ozone is more than 70% greater than the ozonesonde values, whereas this error is reduced by over 50% when EOS MLS data are also assimilated. In addition, the error standard deviation for MLS is reduced by up to 40% compared with the other two runs.

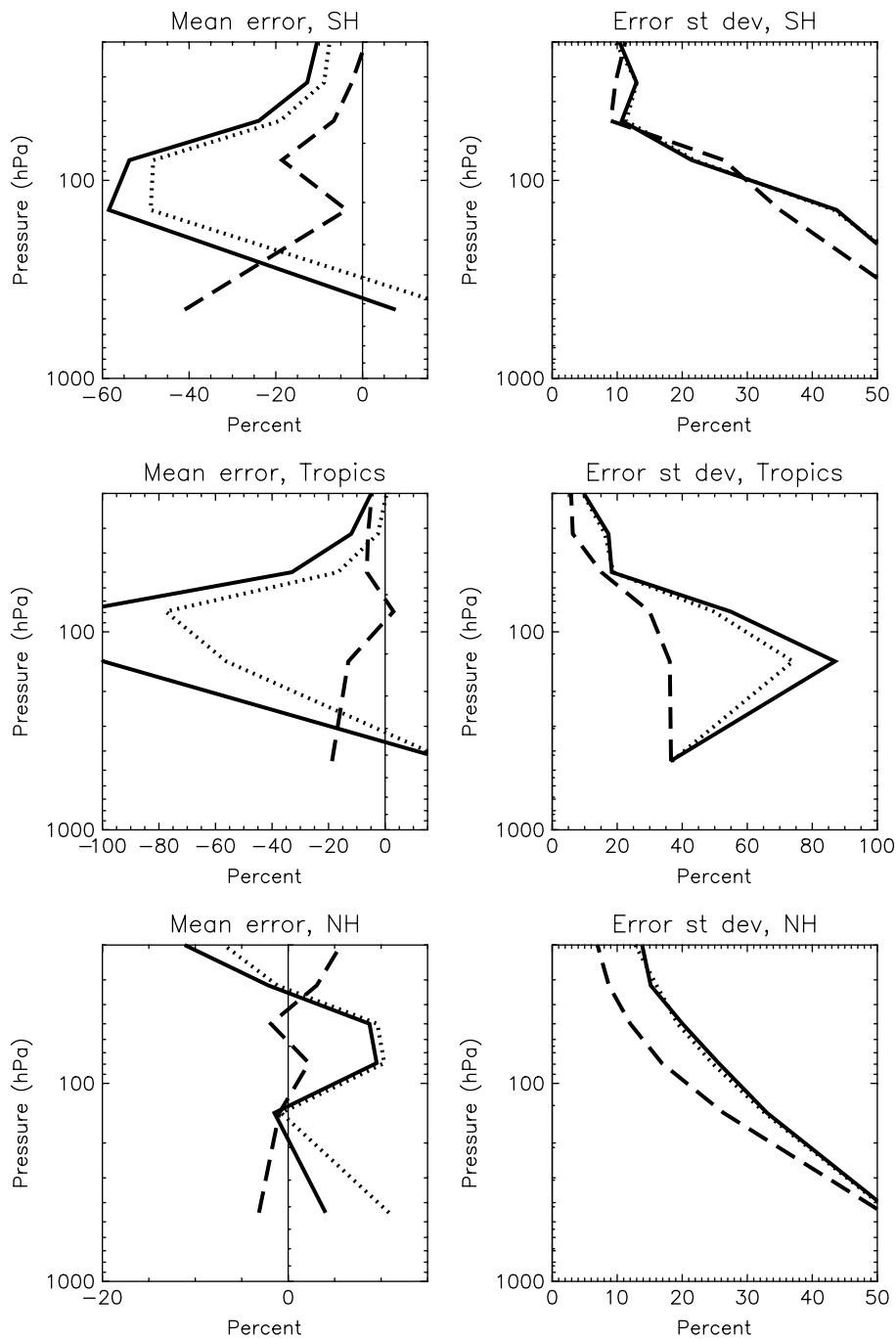


Figure 2. Analysis errors (with respect to ozonesonde data) for the runs CTRL (solid lines), SBUV (dotted lines), and MLS (dashed lines). The errors are normalized by the independent data and are expressed as a percentage. Errors for the Southern-Hemisphere extratropics (30°S – 90°S), the Tropics (30°N – 30°S) and the Northern-Hemisphere extratropics (30°N – 90°N) are shown in the upper, middle and lower panels, respectively; the mean and standard deviation of the errors are shown in the left and right columns, respectively. For the mean errors, positive values indicate that the analysed ozone is less than the observed ozone.

Compared with HALOE (Figure 3), the error mean and standard deviation in the lowermost tropical stratosphere is also smaller in MLS. However, the HALOE data quality degrades in the troposphere, and so no high-quality data are available for comparison below 20 km. In this instance, it is useful to also calculate analysis errors with respect to EOS MLS data. Although these data are included in MLS, their latitudinal coverage is much greater than for the ozonesonde and HALOE data, and therefore a better assessment of the errors in the Tropics can be

made. A comparison of these errors for MLS and CTRL (Figure 4) shows that there is a reduction of up to 80% in the mean error and the error standard deviation in the tropical UTLS. The errors for MLS in this region are also considerably smaller than those for SBUV (not shown).

Above the middle stratosphere (35 km, or 10 hPa), Figure 1 shows little difference between the three analyses, except in northern polar latitudes, where ozone is 0.1–0.2 ppmv lower in MLS. This may indicate the effect of downward transport of low ozone from higher

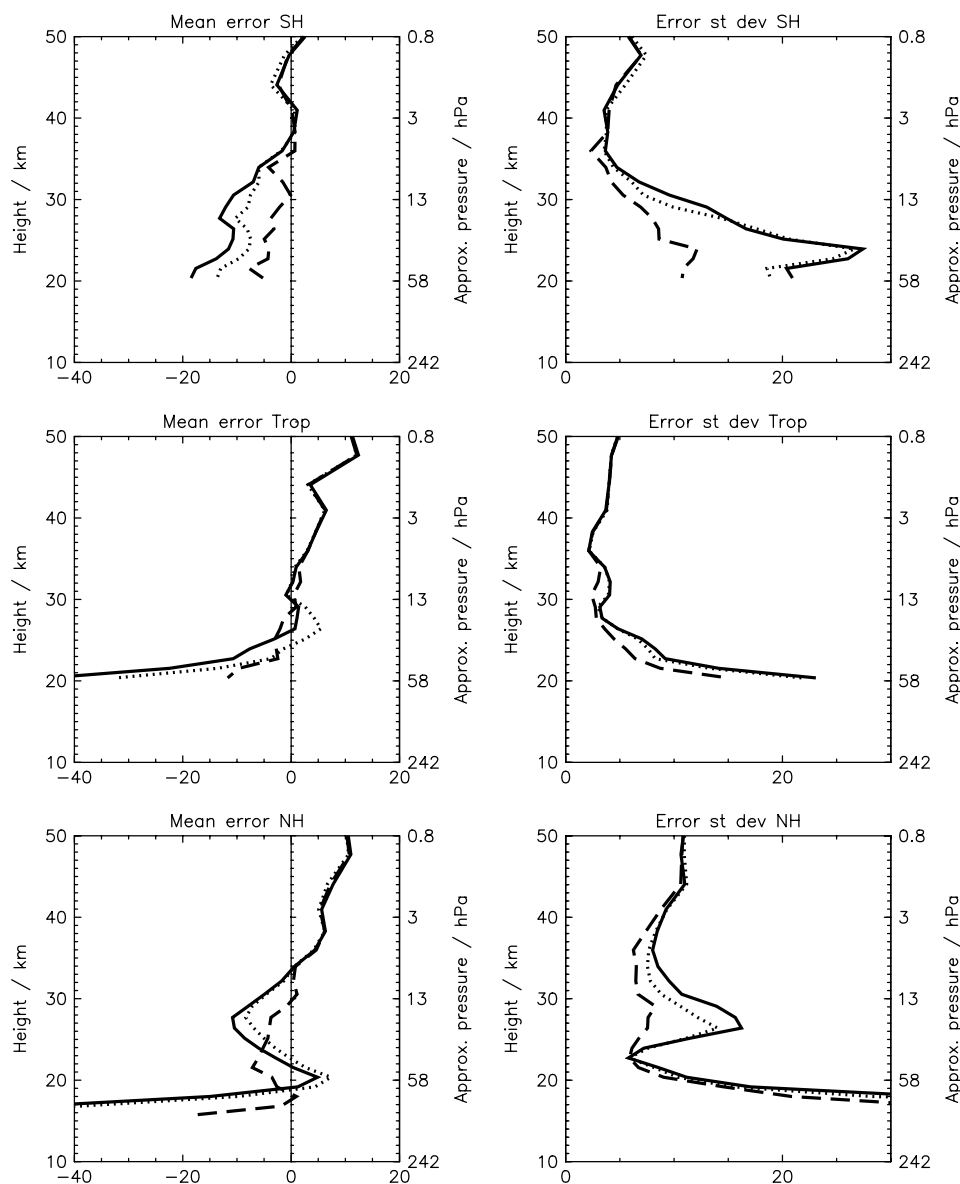


Figure 3. Analysis errors (with respect to HALOE data) for the runs CTRL (solid lines), SBUV (dotted lines), and MLS (dashed lines). The errors are normalized by the independent data and are expressed as a percentage. Errors for the Southern-Hemisphere extratropics (30°S – 90°S), the Tropics (30°S – 30°N) and the Northern-Hemisphere extratropics (30°N – 90°N) are shown in the upper, middle and lower panels, respectively; the mean and standard deviation of the errors are shown in the left and right columns, respectively. For the mean errors, positive values indicate that the analysed ozone is less than the observed ozone. The Southern-Hemisphere and Tropics plots are compared to HALOE sunrise data, and the Northern-Hemisphere plot to HALOE sunset data.

levels, associated with the downward branch of the Brewer–Dobson circulation. It is possible that this transport is not accurately represented in the forecast model. At other latitudes, photochemical changes in ozone would dominate over transport-induced changes, but in the polar night chemical lifetimes are very long (e.g. McCormack *et al.*, 2006; Geer *et al.*, 2007). These differences in ozone have small impacts on HALOE and EOS MLS errors (Figures 3 and 4, respectively) at these levels, the most obvious being a reduction in HALOE error standard deviation.

4.2. Low-ozone events in the southern polar stratosphere

Orsolini *et al.* (2003) and Orsolini and Nikulin (2006) have documented LOEs in the northern summer polar

stratosphere. Summertime ozone loss via gas-phase chemistry is dominated by nitrogen and hydrogen catalytic cycles, which are very efficient at very high latitudes because of the long summer insolation. These chemical conditions, combined with relatively quiet dynamical conditions, allow a low ozone pool of air to form (see also (Lahoz *et al.*, 2007)). After formation, this low ozone can be transported to lower latitudes by planetary-wave activity. Note that this transport can take place in the mid-stratosphere (e.g. 30 hPa) above the zero-wind line (Orsolini and Nikulin, 2006).

Transient column-ozone reductions occur in both hemispheres and in all seasons in anticyclonic conditions associated with an elevated tropopause. Such LOEs, or ozone mini-holes, were first observed in the Southern

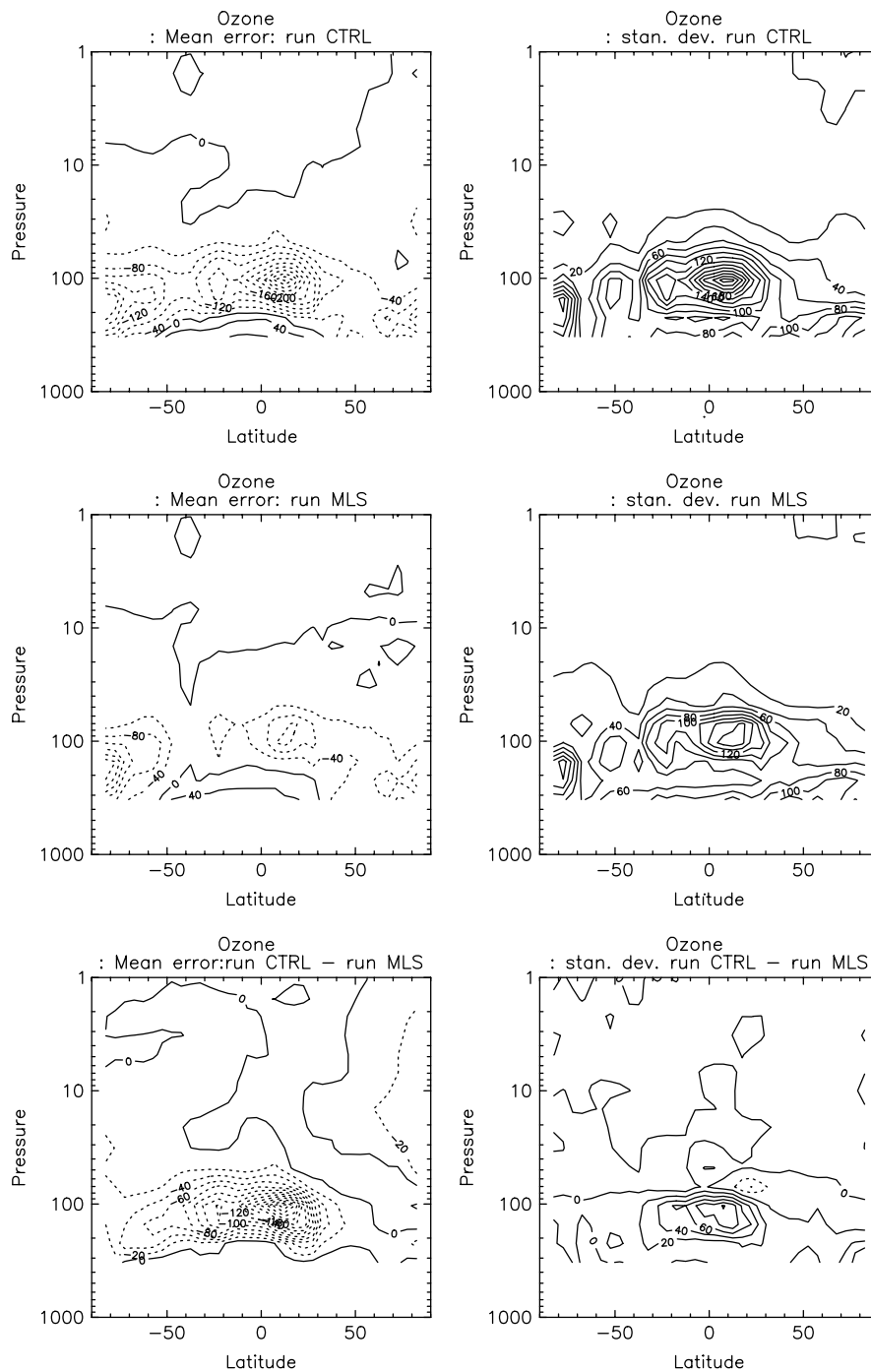


Figure 4. Analysis errors (with respect to EOS MLS data) for the runs CTRL (upper panels) and MLS (middle panels), and the difference between these runs (lower panels). The errors are normalized by the independent data and are expressed as a percentage. The mean and standard deviation of the observation-minus-analysis values are shown in the left and right columns, respectively. The errors are averaged over the period from 26 January to 24 February 2005. The contour interval is 20%.

Hemisphere, and are prominent in the winter. Only recently have summertime LOEs been studied. These column-ozone reductions are accentuated when the pool of low-ozone polar air moves aloft of the tropospheric anticyclone, and the conjunction of these two events (high tropopause and equatorward displacement of the low-ozone polar pool) can give rise to extreme LOEs.

The summer Southern-Hemisphere LOEs produced by MLS have many similarities to the events reported by Orsolini *et al.* (2003). Figure 5 illustrates how each of

the analyses represents the LOE, using the example of analysed ozone at 31 hPa on 11 February 2005. For MLS, ozone over the pole is less than 2.0 ppmv, and tongues of low ozone extending to lower latitudes indicate the transport of low-ozone polar air by planetary waves. The Ertel potential vorticity (PV) field at 650 K, which is close to the 31 hPa level, indicates that the location of the low-ozone tongues over South America and near New Zealand is consistent with the atmospheric flow. Similar features are seen on all other days in MLS. The

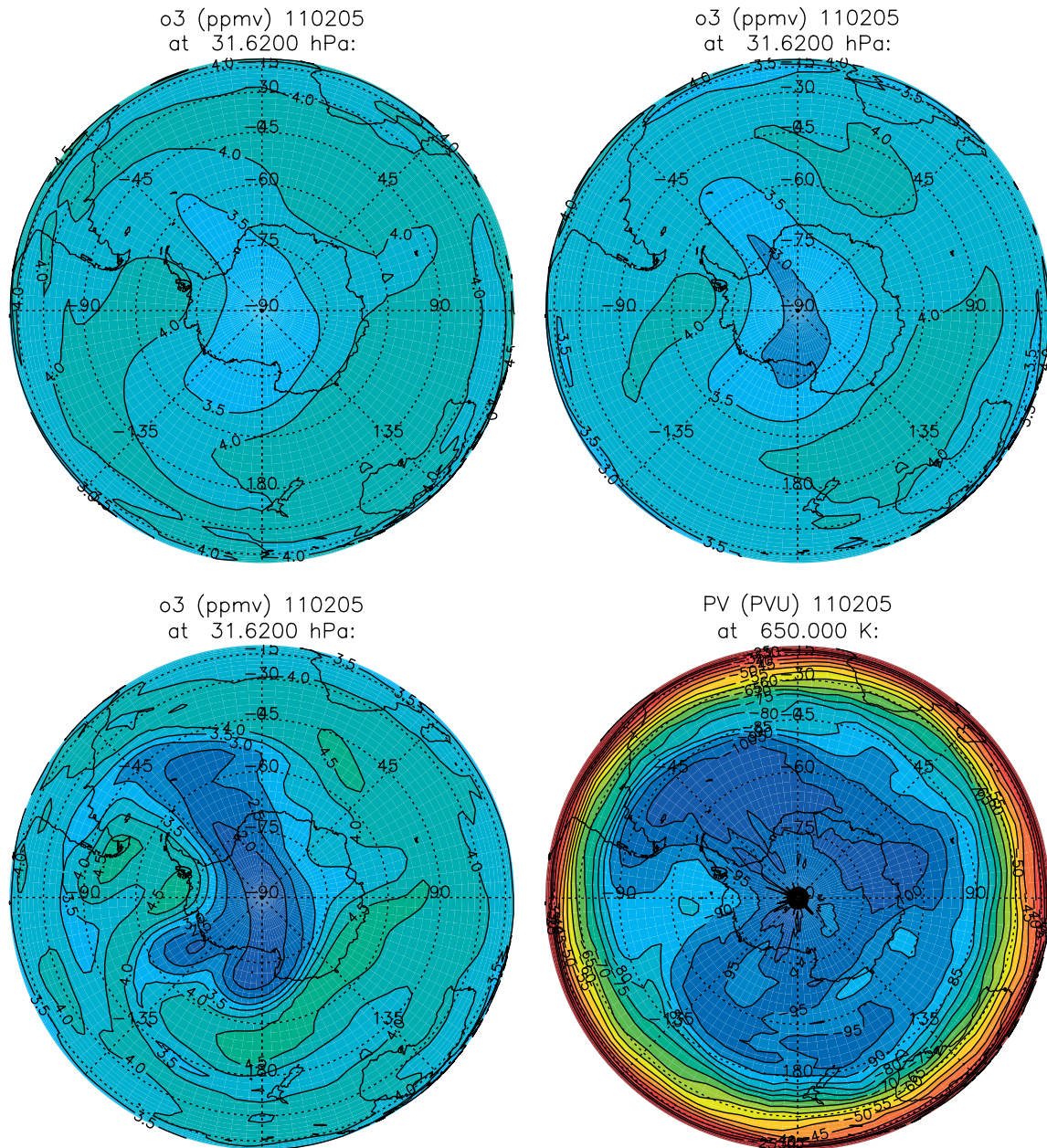


Figure 5. Ozone at 31 hPa on 11 February 2005: runs CTRL (top-left), SBUV (top-right), and MLS (bottom-left). Also shown is Ertel PV at 650 K on 11 February 2005 (bottom-right). Contour intervals: 0.5 ppmv for the ozone plots, 5PVU for the PV plot. This figure is available in colour online at www.interscience.wiley.com/qj

location of these tongues varies from day to day, also indicating the dynamical transport that is taking place. The structure of the ozone field for CTRL in Figure 5 is quite similar to that for MLS. However, polar ozone values are higher, being no less than 3.0 ppmv, and the ozone in the tongues is also greater. In addition, these tongues become increasingly more smeared (compared with MLS) further away from the pole. This suggests that the transport in the analysed wind fields is good enough to represent the mid-stratospheric contribution to the LOE, but that the model ozone photochemistry parametrization scheme does not adequately represent the chemical loss in the polar low-ozone pool.

Figure 5 also shows ozone analyses from SBUV. Ozone over the pole is less than 3.0 ppmv, so the analysis is

doing a reasonable job of representing the LOE, but it is not as deep as in MLS. However, the tongues of low-ozone air extending to lower latitudes are poorly represented. This suggests that these tongues have a finer vertical structure than the low-ozone feature over the pole (a fact confirmed by examination of ozone analyses at adjacent lower-stratospheric levels), and that the assimilation of the low-vertical-resolution SBUV data acts to smear out these tongues. This may be because the ozone background-error covariances, which distribute the observation increments in the vertical, are not sufficiently well represented.

Moreover, the location of the tongues of mid-latitude low ozone will slowly vary with time as they are transported, although the total-ozone field will also

change in time because of the faster, large-amplitude tropopause-level fluctuations. A comparison of the temporal correlation between observed and analysed total-ozone fields is thus an excellent way of validating the analyses.

Figure 6 compares total ozone from the three analyses with TOMS data, for a selection of Southern-Hemisphere locations. All three analyses have higher total ozone than TOMS. This may be because of errors in the tropospheric ozone analysis, since model errors are likely to be larger there and little or no tropospheric ozone observations are assimilated. The bias for CTRL is larger than for the

other two runs. For some locations, MLS seems to spin up faster than SBUV, so that in the first half of the run the former analysis is much closer to TOMS whereas in the second half the two analyses are quite similar. Table I shows the temporal correlation between TOMS and analysed total ozone, at the same locations as are used in Figure 6. In general, the temporal correlation between MLS and TOMS observations is considerably better than for the other runs. An exception to this is over Argentina, where the correlation at Buenos Aires is worse, and that at Comodoro Rivadavia and Ushuaia only slightly better. In general, Figure 6 and Table I suggest that MLS

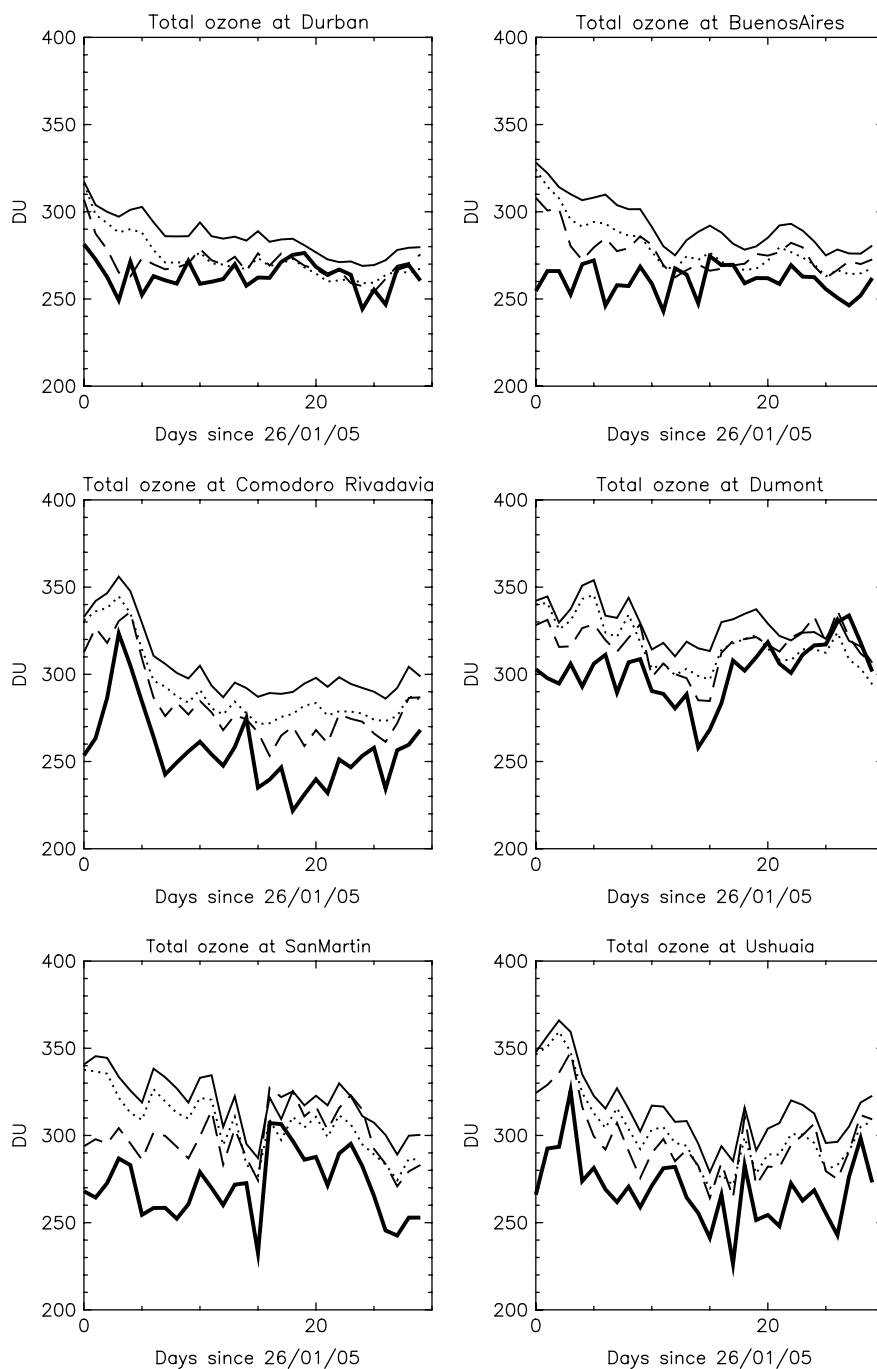


Figure 6. Time series of TOMS total ozone (thick solid lines), and total ozone from runs CTRL (thin solid lines), SBUV (dotted lines) and MLS (dashed lines), for selected Southern-Hemisphere locations. The latitudes and longitudes of these locations are given in Table I.

Table I. Temporal correlations between TOMS total ozone and total ozone from runs CTRL, SBUV and MLS. Correlations that are significant at the 99% level are shown in bold.

Station	CTRL	SBUV	MLS
Durban (30.03°S, 30.98°E)	0.307039	0.315913	0.550679
Buenos Aires (34.58°S, 58.48°W)	0.148465	0.126044	0.038284
Comodoro Rivadavia (45.80°S, 67.50°W)	0.782571	0.742811	0.815503
Ushuaia (54.90°S, 68.30°W)	0.761555	0.725076	0.830977
Dumont d'Urville (66.07°S, 140.02°E)	0.232608	0.272033	0.748554
San Martin (68.13°S, 67.11°W)	0.372781	0.322257	0.891091

does a good job of representing ozone fluctuations at very high latitudes, but that the transport of low ozone values to lower latitudes is represented less well over Argentina than over other locations. Also interesting is that the correlation between TOMS and SBUV is often poorer than that between TOMS and CTRL. Together with the results from Figures 5 and 6, this indicates that the assimilation of SBUV retrievals can degrade the LOE structure preexisting in the background field.

4.3. Northern-Hemisphere polar ozone depletion

The 2004–2005 Arctic winter was very cold in the lower stratosphere. The winter mean PSC volume was the largest on record (Rex *et al.*, 2006), and the period for which 50 hPa temperatures were low enough for Type-I PSC formation was the longest on record (Manney *et al.*, 2006). Thus the potential for significant stratospheric ozone depletion was large. Estimates of lower-stratospheric ozone loss between early January and mid-March 2005 vary between 30% and 60% (e.g. Jin *et al.*, 2006; Rex *et al.*, 2006; von Hobe *et al.*, 2006; Manney *et al.*, 2006). Here, it is illustrated that adding EOS MLS data to the assimilation system improves the ability of the assimilation system to represent such polar ozone depletion.

Figures 1–4 illustrate that ozone in the northern extratropical stratosphere is lower in MLS than in the other two runs, and that the errors in this region are also smaller in MLS. This is because of the different representations of the ozone depletion due to heterogeneous chemistry in the three runs. No parametrization of such ozone loss appears in the forecast model, and so CTRL does not represent this loss at all. In the other two runs, such loss is represented via the assimilated SBUV and EOS MLS data, and MLS does a better job of analysing this ozone loss than does SBUV. We illustrate this further via Figure 7, which shows Northern-Hemisphere ozone on the 750 K isentropic surface (approximately 15 hPa, or 30 km) on 21 February 2005, for the three assimilation trials. Also shown is the corresponding PV field for MLS. (Note that this field is almost identical in all three runs, because ozone/radiation interaction is omitted). The polar vortex is indicated by the areas of strong horizontal gradient in the PV field. Ozone fields on isentropic surfaces tend to show strong correlations with the corresponding PV fields (e.g. Allaart *et al.*, 1993). In MLS, this is clearly the

case, since the shape of the polar vortex in the PV field is quite well reproduced in the ozone field, with lowest ozone values (less than 4.5 ppmv) inside the vortex and a strong horizontal gradient near the vortex edge. This suggests that heterogeneous ozone destruction is taking place largely within the vortex, where temperatures are lowest, and that the strong gradient of PV at the vortex edge is inhibiting transport of this ozone-poor air out of the vortex.

For SBUV, the ozone field at high latitudes is somewhat similar to that of MLS, but the ozone gradient at the vortex edge is weaker, and ozone mixing ratios within the vortex are generally higher. At very high latitudes, the solar zenith angle is very high, and hence many of the SBUV data are blacklisted by the assimilation scheme. This fact, together with the poorer vertical resolution of SBUV compared with EOS MLS, seems to explain this poorer representation of ozone loss. In CTRL, the horizontal ozone gradients seen in MLS and SBUV are absent. This is not surprising, since the only representation of polar ozone loss in CTRL will be from the climatology used to initialize the run. This will be negligible, since that climatology is a zonal-mean monthly mean and is chiefly derived from 1980s data. However, for CTRL, the lowest ozone values are seen over the northern Pacific and northern Atlantic, and the shape of these features bears some resemblance to the low-ozone features seen in MLS and SBUV. These patterns indicate the mean diabatic descent that the initial ozone field has undergone since the start of the run.

The quality of the ozone analysis can also be illustrated by comparing ozone profiles from the analyses and from ozonesonde measurements. Figure 8 shows ozone profiles at Ny Aalesund and Prague on 21 February 2005. At Ny Aalesund, the ozonesonde profile in the lower stratosphere indicates both ozone depletion and smaller-scale vertical structure. This may be due to the presence of gravity waves, or to the transport of laminae of ozone within the vortex. The MLS run represents the ozone depletion and small-scale structure very well, but SBUV fails to represent these features (as does CTRL, which is similar to SBUV, but is omitted from Figure 8 for clarity). For the Prague profile, we focus on the region above 30 hPa. As indicated by Figure 7, this region is located near the edge of the polar vortex on this day, and MLS shows a strong horizontal gradient in ozone near Prague. Figure 8 suggests that the location and strength of this gradient is correct, since the agreement between sonde

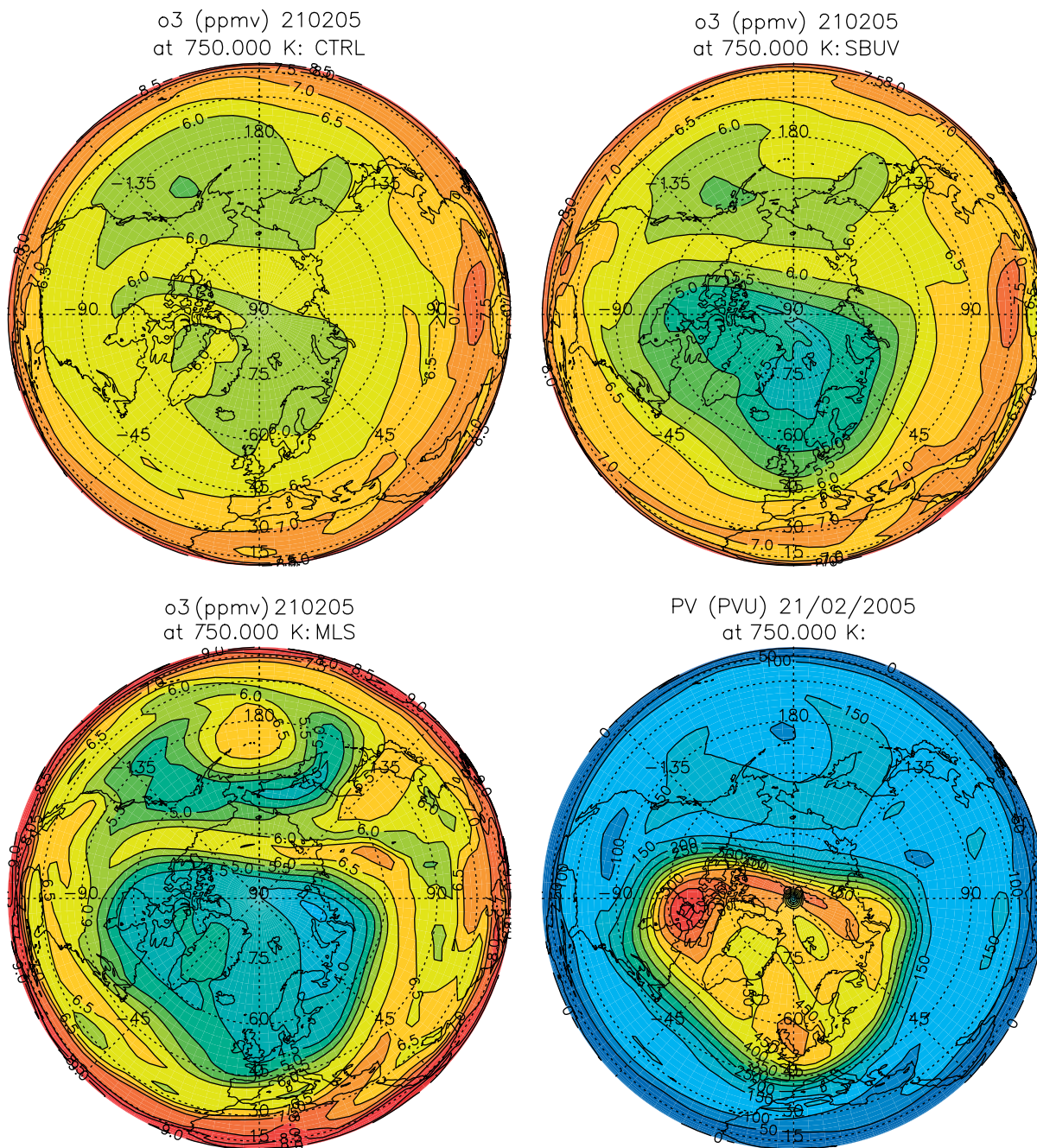


Figure 7. Ozone on the 750 K isentropic surface on 21 February 2005: runs CTRL (top-left), SBUV (top-right), and MLS (bottom-left). Also shown is the Ertel PV field at 750 K (bottom-right). This figure is available in colour online at www.interscience.wiley.com/qj

and MLS ozone is very good. Figure 7 also shows that the gradient in ozone near Prague is weaker in SBUV, and nearly zero in CTRL. The underestimation of the gradient means that ozone over Prague in these two runs is too large (as seen for SBUV in Figure 8).

4.4. Tropical UTLS

Figure 2 shows that analysed ozone near the tropical tropopause is overestimated by more than 70% in CTRL and SBUV, and that this bias is reduced by over 50% when EOS MLS data are also assimilated. The standard deviation of these errors is also much smaller

in MLS than in the other two runs. In similar experiments where MIPAS ozone profiles are assimilated, Geer *et al.* (2006a) report that ozone near the tropical tropopause is overestimated by around 40%. Therefore, it appears that EOS MLS data have a larger benefit than MIPAS data for the quality of the ozone analysis in this region. EOS MLS and MIPAS observation errors are generally quite similar in this region – MIPAS observation errors below 20 km are 5%–10% (random) and 8%–20% (total) (Raspollini *et al.*, 2006), and the EOS MLS retrieval accuracy is around 5%–10% in the stratosphere and considerably higher in the upper troposphere (Livesey *et al.*, 2005) – so this is unlikely to explain the

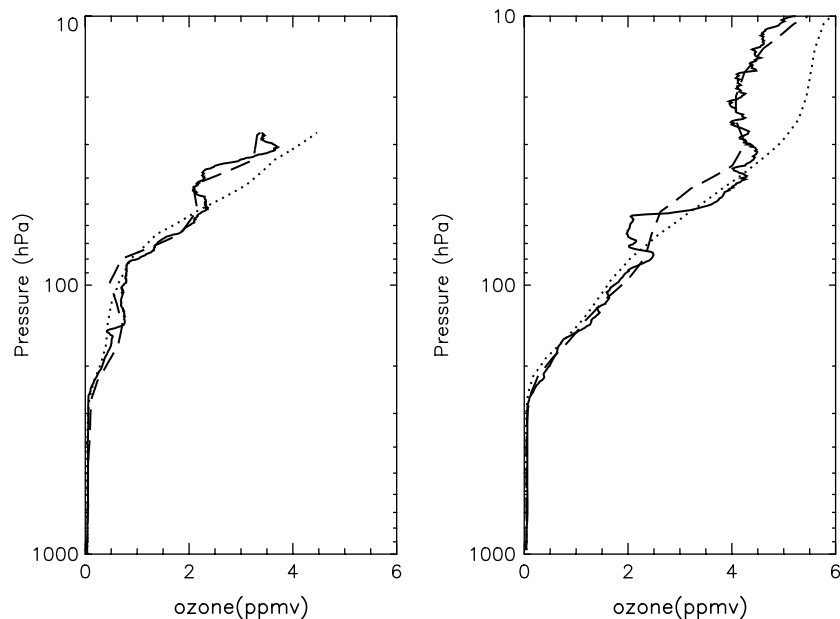


Figure 8. Ozone profiles from ozonesonde observations (solid lines), run SBUV (dotted lines), and run MLS (dashed lines), on 21 February 2005, at Ny Aalesund (78.93°N, 11.95°E) (left) and at Prague (50.01°N, 14.45°E) (right).

differences between the EOS MLS and MIPAS analyses. However, MIPAS retrieval profiles are reportedly rather noisy (e.g. Geer *et al.*, 2006a), and this may degrade the quality of the ozone analysis.

Another possible reason for the difference between the MIPAS and EOS MLS ozone analyses is that there are 4–5 times as many EOS MLS observations as MIPAS observations per day. A further assimilation trial was run in which only a quarter of the EOS MLS observations were used in the assimilation. This was done to approximate the MIPAS data coverage. However, the results were nearly identical to those for MLS; therefore the good performance of MLS near the tropical tropopause is not related to the greater density of EOS MLS observations.

Next, we further investigate the differences between the MLS analyses and the CTRL and SBUV analyses in the tropical UTLS. Geer *et al.* (2006a) attribute the poor tropical UTLS ozone analyses to poor transport. It is well known that tropical wind analyses can be poor (e.g. Žagar, 2004), and the effect of these winds when used to transport atmospheric tracers can be to produce excessive horizontal mixing between the Tropics and the extratropics and excessive vertical mixing between the UTLS and higher stratospheric levels (e.g. Schoeberl *et al.*, 2003). Much of the degradation in the tropical wind analyses is believed to be related to the erosion of mass–wind balance that can happen during data assimilation when an analysis increment is added to a well-balanced background field. Thus, to assist in our investigation we also look at the performance of a long model forecast run (MOD). This run is initialized on 25 January 2005 with the same data as for the assimilation runs, and a 30-day forecast, without any data assimilation, is run through to 24 February 2005.

The zonal-mean structure of the MOD ozone field near the tropopause (not shown) is similar to that for CTRL and SBUV (Figure 1). The vertical gradient here is weaker than for MLS; this may indicate excessive transport of ozone across the tropopause. Comparisons with ozonesonde data (not shown) indicate that, like the ozone in CTRL and SBUV, MOD ozone is greatly overestimated in the tropical tropopause region.

Focusing now on the horizontal structure, Figure 9 shows analysed and model ozone fields at 100 hPa at low latitudes on 13 February 2005. This figure shows that the ozone in MOD, CTRL and SBUV in this region is clearly greater than in MLS; this is consistent with previous figures, which show that the former runs overestimate ozone here far more than MLS does. The MOD and MLS fields at the Equator are fairly uniform, but the level of zonal asymmetry in the CTRL and SBUV fields is much larger. This is confirmed by the fact that the standard deviation of ozone at low latitudes is around twice as large for CTRL and SBUV as for MOD and MLS. Note that this pattern of differences between the runs is seen on most days in the analysis period, not just 13 February 2005.

The increased variance in CTRL and SBUV is largely a result of the emergence of relatively small-scale features, such as the very low ozone east of Africa and in the equatorial Pacific and increased ozone over northern Australia. These features are not present in MOD or MLS. An examination of temperature fields at 100 hPa shows that east of Africa and in the equatorial Pacific the are also low temperatures that are indicative of tropical convection and ascent. In all the assimilation runs, the temperature in these regions is more than 5 K lower than in MOD, and has considerably more localized structure. It is assumed that this structure is related to the erosion of

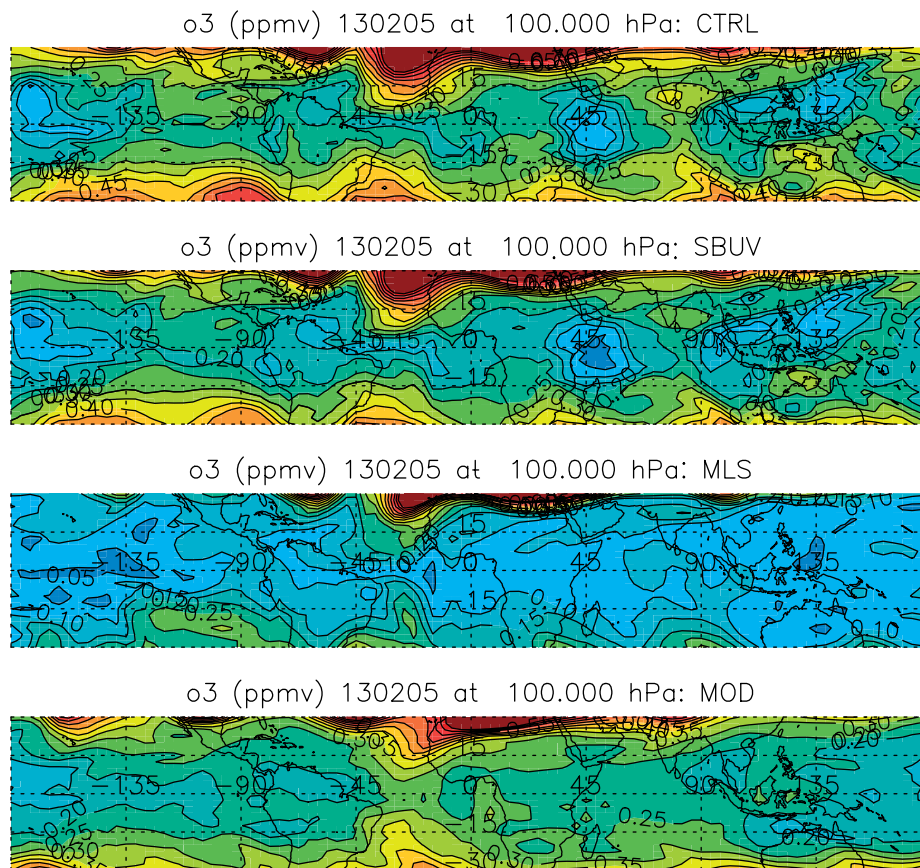


Figure 9. Ozone at 100 hPa between 30°S and 30°N on 13 February 2005, from runs (top to bottom) CTRL, SBUV, MLS, and MOD. The contour interval is 0.05 ppmv; high ozone is shown in red and low ozone in blue. This figure is available in colour online at www.interscience.wiley.com/qj

balance in the assimilation runs. The regions of localized low temperature in the assimilation runs also indicate that ascent there is likely to be stronger, and the transport of ozone-poor air from lower levels to 100 hPa will be greater, and also more localized. This explains the localized regions of low ozone seen east of Africa and in the equatorial Pacific in CTRL. Since ozone errors for this run are high in this region, it is assumed that these features are erroneous. The presence of such low-ozone features in SBUV indicates that the assimilated SBUV data are too sparse to correct these low ozone amounts, or indeed to address the bias present in the background ozone field. In MLS, however, the greater quantity and higher vertical resolution of the assimilated EOS MLS data mean that the associated analysis increments remove the low, erroneous, ozone features seen in CTRL and SBUV.

Since the mean and standard deviation of the MLS ozone errors in the Tropics at 100 hPa are considerably smaller than for the other runs, it is reasonable to assume that the MLS structure in Figure 9 is closer to reality than that of the other three runs. The fairly uniform structure of the MLS ozone field around the Equator at 100 hPa concurs with studies such as (Thompson *et al.*, 2003), which shows that the observed ozone field in the equatorial UTLS has a fairly small zonal variance. Therefore it is reasonable to conclude that the low-ozone features seen in CTRL and SBUV, for example east of Africa, are erroneous

and related to a lack of balance between the analysed mass and wind fields. The assimilation of EOS MLS data strongly reduces the analysis error associated with these features, as well as any larger-scale errors arising from the background ozone field.

4.5. Results from other periods

Ideally, CTRL, SBUV and MLS would be run for different seasons and years in order to investigate how the impact of EOS MLS observations on the ozone analyses is influenced by seasonal and interannual variability. Unfortunately, the computational expense of data-assimilation trials makes this unfeasible. Instead, MLS has been run for two further periods: 2–31 January 2006 and 5–30 June 2006. In Figure 10, mean errors (with respect to ozonesonde observations) for these runs are compared to CTRL and MLS errors for the period 26 January to 24 February 2005. Note that in this figure the errors for the winter and summer extratropics are plotted on the same panels. For the summer extratropics and the Tropics, the MLS errors for all three periods are fairly similar, and are considerably smaller than the CTRL errors, particularly in the UTLS region. The standard deviations of the errors for MLS are also smaller than for CTRL (not shown), in general. These results suggest that the good representation of the summer stratosphere LOEs and of the tropical UTLS ozone structure seen in January–February 2006 in

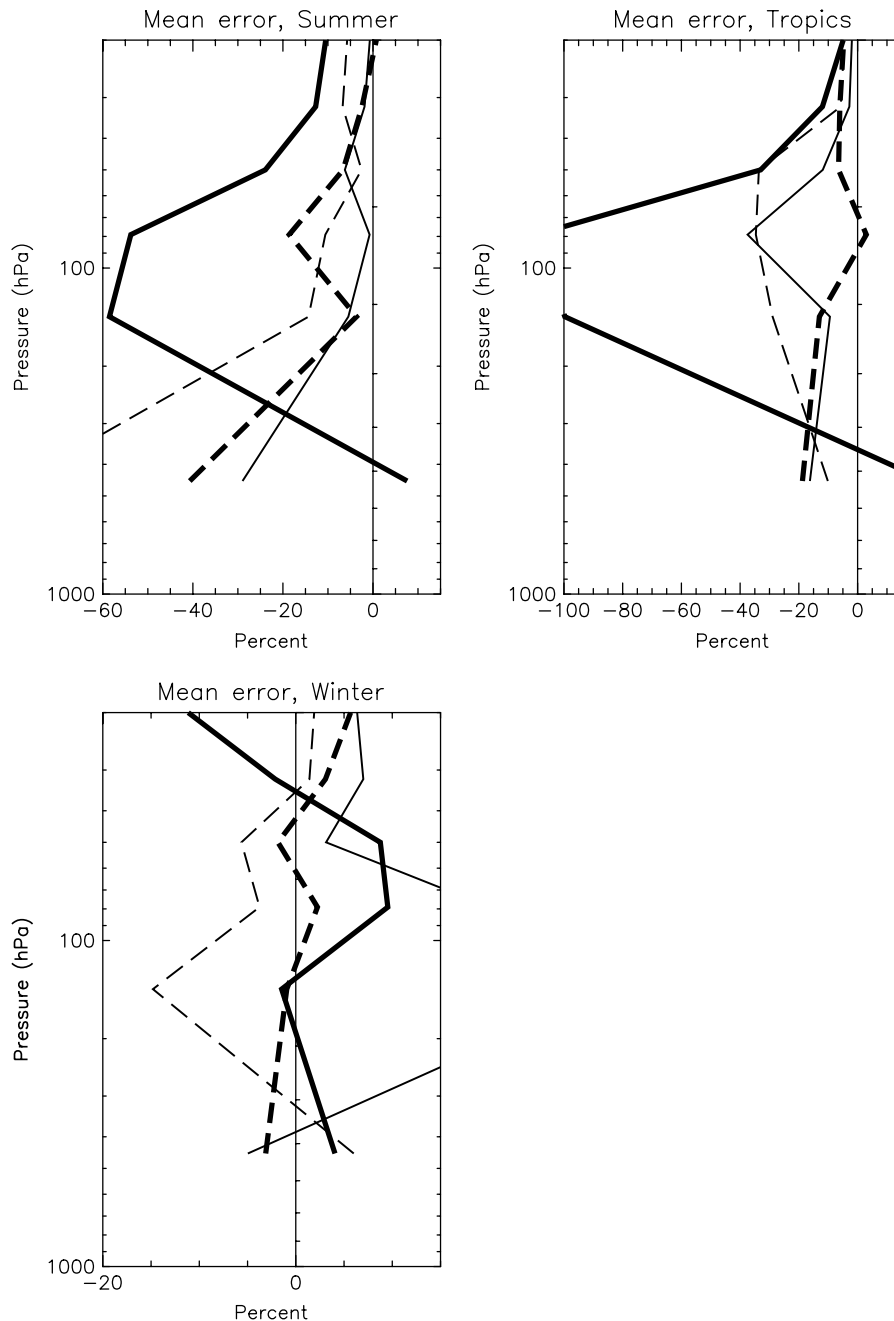


Figure 10. Mean analysis errors (with respect to ozonesonde data), for the runs CTRL (thick solid lines) and MLS (thick dashed lines), for the period 26 January to 24 February 2005, run MLS for the period 2–31 January 2006 (thin dashed lines), and run MLS for the period 5–30 June 2006 (thin solid lines). The errors are normalized by the independent data and are expressed as a percentage. Errors for the Southern-Hemisphere extratropics (30°S – 90°S), the Tropics (30°N – 30°S) and the Northern-Hemisphere extratropics (30°N – 90°N) are shown in the top-left, top-right and bottom panels, respectively. Northern-Hemisphere (Southern-Hemisphere) extratropical errors for the period 5–30 June 2006 are plotted next to the Southern-Hemisphere (Northern-Hemisphere) extratropical errors for the other periods. Positive values indicate that the analysed ozone is less than the observed ozone.

MLS (as discussed in Sections 4.2 and 4.4) is not just a one-off, but occurs in all three periods examined.

For the winter extratropics, it can be seen that the mean errors in January–February 2005 and 2006 in MLS in the lower stratosphere are fairly similar, and are generally smaller than the errors for CTRL. This suggests that the addition of EOS MLS data to the assimilation also improves the analysis of polar ozone depletion in 2006. For June 2006, the mean errors of MLS above 50 hPa are also fairly similar to those in January. However, below

50 hPa the mean error is much larger than for all other runs, indicating a potential problem in the assimilation at these levels which may merit further investigation.

5. Conclusions

In this paper we have demonstrated the benefits of adding EOS MLS ozone profiles to the Met Office ozone data-assimilation system. When EOS MLS observations

are included, mean analysis errors, and the analysis error standard deviation, are found to be considerably smaller than in other runs where only SBUV ozone data are assimilated (SBUV), or where no ozone data are assimilated (CTRL). Compared with the latter runs, mean errors for MLS drop by 5%–25% in the Southern-Hemisphere extratropical stratosphere, by around 10% in the Northern-Hemisphere extratropical stratosphere, and by around 50% (with respect to ozonesondes) in the tropical UTLS. Such reductions in errors indicate the high quality of the EOS MLS dataset. The experiments have been run using version 1.51 or version 1.52 EOS MLS retrievals. These have recently been superseded by version 2.2 retrievals, which typically have smaller errors. Repeating the assimilation experiments with version 2.2 data could lead to even better results than those presented here.

Further investigation shows that the improved ozone analyses in the Southern Hemisphere largely result from a much better representation of summertime LOEs. The structure of these phenomena has been documented by Orsolini *et al.* (2003) in a study of LOEs in the northern summer stratosphere. This is the first time that summer LOEs in the southern stratosphere have been reported. These LOEs are present in MLS for both January–February 2005 and January 2006 (latter results not shown). A full examination of the LOEs in both years will appear in a later paper. Typically, in the lower stratosphere one sees low ozone over the pole and tongues of low ozone drawn out to lower latitudes. The tongues appear because of the transport of the ozone-poor polar air by planetary waves. Both MLS and CTRL reproduce this structure well, but the depth of the LOE is underestimated in CTRL. This suggests that the model's ozone photochemistry parametrization scheme does not adequately represent the chemical ozone loss within the summer low-ozone polar pool. In contrast to MLS and CTRL, SBUV fails even to adequately represent the structure of the LOEs. It appears that the low vertical resolution of the SBUV data assimilated leads to a smearing of any realistic ozone structure present in the background field. This smearing is likely to be related to the specification of the ozone background-error covariances. This is a difficult problem to overcome in data assimilation, but it appears that the high horizontal and vertical resolution of the EOS MLS data, and their low biases, mean that this problem can be circumvented.

In the Northern Hemisphere, the addition of EOS MLS data to the assimilation system leads to a better representation of winter polar ozone depletion. Comparison of analysed and ozonesonde profiles at various locations indicates that MLS in particular does well in representing the strong gradient of ozone near the vortex edge. Such a gradient is underestimated in the other two runs.

In the tropical UTLS, the assimilation of EOS MLS data leads to a better representation of the strong vertical gradient in ozone between the upper troposphere and the lower stratosphere. The ozone analysis in this region can be adversely affected by model transport errors,

and indeed the horizontal structure of ozone fields here in CTRL and SBUV appears to be too noisy. The ozone transport errors probably result from a lack of balance in the assimilated mass and wind fields. The addition of high-density, good-quality EOS MLS data alleviates much of this error.

Furthermore, the MLS ozone analysis errors in the tropical UTLS are considerably smaller than errors from similar experiments made using MIPAS data (Geer *et al.*, 2006a). This may be because there is less vertical noise in the EOS MLS ozone profiles. The MIPAS data are generally considered to be a high-quality, very useful, dataset, so this result underlines how good the EOS MLS ozone retrievals are. Another point not considered is that the MIPAS experiments of (Geer *et al.*, 2006a) were run for the period July–November 2003, whereas we focus on EOS MLS results for January–February 2005. Therefore, it is possible that interannual and seasonal variability may account for the differences in the EOS MLS and MIPAS results. This is hard to test rigorously, since the observational datasets are generally not both available for overlapping periods. However, we show in Section 4.5 that most of the MLS errors are similar whether the assimilation is run for January–February 2005, January 2006 or June 2006. This shows us that the results presented here are robust. Of course, a more complete assessment of the impact of EOS MLS data on our ozone analyses would require assimilations to be run for other seasons and longer periods. However, the computational expense of this makes it difficult to achieve quickly.

This paper also serves to highlight some of the existing weaknesses in the ozone assimilation system. These include ozone transport errors resulting from the erosion of mass–wind balance when analysis increments are added to the system, and the inaccurate distribution of SBUV analysis increments in the vertical, which is associated with the specification of the ozone background-error covariance, and which results in the smearing of features in the ozone field such as the tongues of ozone-poor air drawn into lower latitudes after an LOE. Work is ongoing to address such problems. This work includes developing a 4D-Var version of the ozone-assimilation scheme, which may be better equipped to preserve mass–wind balance than the current 3D-Var scheme, and work to improve the accuracy of the ozone background-error covariances.

The clear benefit that assimilation of EOS MLS data provides to ozone analyses gives renewed hope that such analyses may lead to improvements in NWP: in particular, improved temperature analyses and forecasts resulting from the ozone/radiation interaction. Cariolle and Morcrette (2006) suggest that ozone observations with a vertical resolution of around 1 km are required in order to properly represent the ozone gradient in the UTLS, and the associated radiative heating due to ozone. The results presented here show that the addition of EOS MLS data considerably improves the analysed ozone gradient in the UTLS. Because of this, the investigation

of the impact of the ozone/radiation interaction on NWP forecasts is now an active area of Met Office research, notwithstanding the fact that the vertical resolution of the EOS MLS profiles is lower than the above figure. Preliminary results show that forecast skill scores are improved slightly when ozone analyses produced using EOS MLS data are used in the forecast model radiation scheme. It is also possible that the better representations of horizontal structure in the ozone field, such as the polar vortex edge, that result from the high-horizontal-resolution EOS MLS observations may feed through to improved analyses and forecasts of surface UV.

Acknowledgements

I thank the International Space Science Institute (ISSI <http://www.issibern.ch>) for support in planning and preparing this paper, and Nathaniel Livesey, Andrew Lorenc, Yvan Orsolini and the two anonymous referees for very useful comments on earlier drafts. EOS MLS Science Team work carried out by the Jet Propulsion Laboratory, California Institute of Technology, was under a contract with the National Aeronautics and Space Administration (NASA). EOS MLS data were downloaded from the NASA Goddard Space Flight Center.

References

- Allaart MAF, Kelder H, Heijboer LC. 1993. On the relation between ozone and potential vorticity. *Geophys. Res. Lett.* **20**: 811–814.
- Austin J, Barwell BR, Cox SJ, Hughes PA, Knight JR, Ross G, Sinclair P, Webb AR. 1994. The diagnosis and forecast of clear sky ultraviolet levels at the Earth's surface. *Meteorol. Appl.* **1**: 321–336.
- Beekmann M, Ancellet G, Megie G, Smit HGJ, Kley D. 1994. Intercomparison campaign for vertical ozone profiles including electrochemical sondes of ECC and Brewer-Mast type and a ground based UV-differential absorption radar. *J. Atmos. Chem.* **19**: 259–288.
- Bhartia PK, Taylor S, McPeters RD, Wellemeyer C. 1995. Application of the Langley plot method to the calibration of the solar backscattered ultraviolet instrument on the Nimbus 7 satellite. *J. Geophys. Res.* **100**: 2997–3004.
- Bhartia PK, McPeters RD, Mateer CL, Flynn LE, Wellemeyer C. 1996. Algorithm for the estimation of vertical ozone profiles from the backscattered ultraviolet technique. *J. Geophys. Res.* **101**: 18 793–18 806.
- Bhatt PP, Remsburg EE, Gordley LL, McInerney JM, Brackett VG, Russell JM. 1999. An evaluation of the quality of Halogen Occultation Experiment ozone profiles in the lower stratosphere. *J. Geophys. Res.* **104**: 9261–9275.
- Bruhl C, Drayson SR, Russell JM, Crutzen PJ, McInerney JM, Purcell PN, Claude H, Gernandt H, McGee TJ, McDermaid IS, Gunson MR. 1996. Halogen occultation experiment ozone channel validation. *J. Geophys. Res.* **101**: 10 217–10 240.
- Cariolle D, Deque M. 1986. Southern-hemisphere medium-scale waves and total ozone disturbances in a spectral general circulation model. *J. Geophys. Res.* **92**: 10 825–10 846.
- Cariolle D, Morcrette J-J. 2006. A linearized approach to the radiative budget of the stratosphere: influence of the ozone distribution. *Geophys. Res. Lett.* **33**: L05806. doi:10.1029/2005GL025597.
- Davies T, Cullen MJP, Malcolm AJ, Mawson MH, Staniforth A, White AA, Wood N. 2005. A new dynamical core for the Met Office's global and regional modelling of the atmosphere. *Q. J. R. Meteorol. Soc.* **131**: 1759–1782.
- Dethof A. 2003. 'Assimilation of ozone retrievals from the MIPAS instrument on board ENVISAT'. ECMWF Technical Memo. 428.
- Dethof A, Holm EV. 2004. Ozone assimilation in the ERA-40 reanalysis project. *Q. J. R. Meteorol. Soc.* **130**: 2851–2872.
- Errera Q, Fonteyn D. 2001. Four-dimensional variational chemical assimilation of CRISTA stratospheric measurements. *J. Geophys. Res.* **106**: 12 253–12 265.
- Eskes HJ, van Velthoven PFJ, Valks PJM, Kelder HM. 2003. Assimilation of GOME total-ozone satellite observations in a three dimensional tracer-transport model. *Q. J. R. Meteorol. Soc.* **129**: 1663–1681.
- Froidevaux L, Livesey NJ, Read WG, Jiang YB, Jimenez CJ, Filipiak MJ, Schwartz MJ, Santee ML, Pumphrey HC, Jiang JH, Wu DL, Manney GL, Drouin BJ, Waters JW, Fetzer EJ, Bernath PF, Boone CD, Walker KA, Jucks KW, Toon GC, Margitan JJ, Sen B, Webster CR, Christensen LE, Elkins JW, Atlas E, Ueb RA, Hendershot R. 2006. Early validation analyses of atmospheric profiles from EOS MLS on the Aura satellite. *IEEE Trans. Geosci. Remote Sensing* **44**: 1106–1121.
- Froidevaux L, Jiang YB, Lambert A, Livesey NJ, Read WG, Waters JW, Browell EV, Hair JW, Avery MA, McGee TJ, Twigg LW, Sunnicht GK, Jucks KW, Margitan JJ, Sen B, Stachnik RA, Toon GC, Bernath PF, Boone CD, Walker KA, Filipiak MJ, Harwood RS, Fuller RA, Manney GL, Schwartz MJ, Daffer WH, Drouin BJ, Cofield RE, Cuddy DT, Jarnot RF, Knosp BW, Perun VS, Snyder WV, Stek PC, Thurstans RP, Wagner PA. 2007. Validation of the Aura Microwave Limb Sounder stratospheric ozone measurements. *J. Geophys. Res.* (submitted).
- Geer AJ, Lahoz WA, Bekki S, Bormann N, Errera Q, Eskes HJ, Fonteyn D, Jackson DR, Juckes MN, Massart S, Peuch V-H, Rharmili S, Segers A. 2006a. The ASSET intercomparison of ozone analyses: method and first results. *Atmos. Chem. Phys.* **6**: 5445–5474.
- Geer AJ, Peubey C, Bannister R, Brugge R, Jackson DR, Lahoz WA, Migliorini S, O'Neill A. 2006b. Assimilation of stratospheric ozone from MIPAS into a global general circulation model: the September 2002 vortex split. *Q. J. R. Meteorol. Soc.* **132**: 231–257.
- Geer AJ, Lahoz WA, Jackson DR, Cariolle D, McCormack JP. 2007. Evaluation of linear ozone photochemistry parametrizations in a stratosphere-troposphere data assimilation system. *Atmos. Chem. Phys.* **7**: 939–959.
- Grooss JU, Russell JM. 2005. Technical Note: A stratospheric climatology for O₃, H₂O, CH₄, NO_x, HCl and HF derived from HALOE measurements. *Atmos. Chem. Phys.* **5**: 2797–2807.
- Holm EV, Untch A, Simmons A, Saunders R, Bouttier F, Andersson E. 1999. Multivariate ozone assimilation in four-dimensional data assimilation. Pp 89–94 in *Proceedings of the SODA Workshop on Chemical Data Assimilation*, 9–10 December 1998, KNMI, De Bilt, The Netherlands.
- Holm EV, Untch A, Simmons A, Saunders R, Bouttier F, Andersson E. 2000. Multivariate ozone assimilation. Pp 305–308 in *Proceedings of the Third International Symposium on Assimilation of Observations in Meteorology and Oceanography*, 7–11 June 1999, Quebec City, Canada, TD 986. WMO, Geneva, Switzerland.
- Jackson DR. 2004. 'Improvements in ozone data assimilation at the Met Office'. Met Office Forecasting Research Technical Report 454.
- Jackson DR, Saunders R. 2002. 'Ozone data assimilation: preliminary system'. Met Office Forecasting Research Technical Report 394.
- Jiang YB, Froidevaux L, Lambert A, Livesey NJ, Read WG, Waters JW, Bojkov B, Leblanc T, McDermaid IS, Godin-Beekmann S, Filipiak MJ, Harwood RS, Fuller RA, Daffer WH, Drouin BJ, Cofield RE, Cuddy DT, Jarnot RF, Knosp BW, Perun VS, Schwartz MJ, Snyder WV, Stek PC, Thurstans RP, Wagner PA, Allaart M, Andersen SB, Bodeker G, Calpini B, Claude H, Coetzee G, Davies J, DeBacker H, Dier H, Fujiwara M, Johnson B, Kelder H, Leme NP, König-Langlo G, Kyro E, Laneve G, Fook LS, Merrill J, Morris G, Newchurch M, Oltmans S, Parrondos MC, Posny F, Schmidlin F, Skrivankova P, Stubi R, Tarasick D, Thompson A, Thouret V, Viatte P, Vomel H, von der Gathen P, Yela M, Zabolocki G. 2007. Validation of the Aura Microwave Limb Sounder Ozone by Ozonesonde and Lidar Measurements. *J. Geophys. Res.* (submitted).
- Kerr JB, Fast H, McElroy CT, Oltmans SJ, Lathrop JA, Kyro E, Paukkunen A, Claude H, Kohler U, Sreedharan CR, Takao T, Tsukagoshi Y. 1994. The 1991 WMO international ozonesonde intercomparison at Vanscoy, Canada. *Atmos.–Ocean* **4**: 685–716.
- Komhyr WD, Barnes RA, Brothers GB, Lathrop JA, Opperman DP. 1995. Electrochemical Concentration Cell ozonesonde performance evaluation during STOIC 1989. *J. Geophys. Res.* **100**: 9231–9244.
- Lahoz WA, Geer AJ, Orsolini YJ. 2007. Northern Hemisphere stratospheric summer from MIPAS observations. *Q. J. R. Meteorol. Soc.* **133**: 197–211.
- Li D, Shine KP. 1995. 'A 4-dimensional ozone climatology for UGAMP models'. UGAMP Int. Rep. 35, April 1995.

- Livesey NJ, Read WG, Filipiak MJ, Froidevaux L, Harwood RS, Jiang JH, Jimenez C, Pickett HM, Pumphrey HC, Santee ML, Schwartz MJ, Waters JW, Wu DL. 2005. 'EOS MLS Version 1.5 Level 2 data quality and description document'. JPL, California.
- Livesey NJ, Filipiak MJ, Froidevaux L *et al.* 2007. Validation of Aura Microwave Limb Sounder O₃ and CO observations in the upper troposphere and lower stratosphere. *J. Geophys. Res.* (submitted).
- Lorenc AC, Ballard SP, Bell RS, Ingleby NB, Andrews PLF, Barker DM, Bray JR, Clayton AM, Dalby T, Li D, Payne TJ, Saunders FW. 2002. The Met. Office global three dimensional data assimilation scheme. *Q. J. R. Meteorol. Soc.* **126**: 2991–3012.
- Manney GL, Santee ML, Froidevaux L, Hoppel K, Livesey NJ, Waters JW. 2006. EOS MLS observations of ozone loss in the 2004–2005 Arctic winter. *Geophys. Res. Lett.* **33**: L04802. doi:10.1029/2006GL026731.
- McCormack JP, Eckermann SD, Siskind DE, McGee TJ. 2006. CHEM2D-OPP: A new linearized gas-phase ozone photochemistry parameterization for high-altitude NWP and climate models. *Atmos. Chem. Phys.* **6**: 4943–4972.
- McPeters RD, Bhartia PK, Krueger AJ, Herman JR, Wellemeyer CG, Seftor CJ, Jaross G, Torres O, Moy L, Labow G, Byerly W, Taylor SL, Swisler T, Cebula RP. 1998. 'Earth Probe Total Ozone Mapping Spectrometer (TOMS) Data Products User's Guide'. NASA Technical Publication 1998–206 895, NASA Goddard Space Flight Center, Greenbelt, Maryland 20771.
- Morcrette J-J. 2003. 'Ozone-radiation interactions in the ECMWF forecast system'. ECMWF Technical Memo. 375.
- Orsolini YJ, Eskes H, Hansen G, Hoppe UP, Kylling A, Kyro E, Notholt J, van der A R, von der Gathen P. 2003. Summertime low-ozone episodes at northern high latitudes. *Q. J. R. Meteorol. Soc.* **129**: 3265–3275.
- Orsolini YJ, Nikulin G. 2006. A low-ozone episode during the European heatwave of August 2003. *Q. J. R. Meteorol. Soc.* **131**: 667–680.
- Raspolini P, Belotti C, Burgess A, Carli B, Carlotti M, Ceccherini S, Dinelli BM, Dudhia A, Flaud JM, Funke B, Hopfner M, Lopez-Puertas M, Payne V, Piccolo C, Remedios JJ, Ridolfi M, Spang R. 2006. MIPAS level 2 operational analyses. *Atmos. Chem. Phys.* **6**: 5605–5630.
- Rex M, Salawitch RJ, Deckelmann H, von der Gathen P, Harris NRP, Chipperfield MP, Naujokat B, Reimer E, Allaart M, Andersen SB, Bevilacqua R, Braathen GO, Claude H, Davies J, De Backer H, Dier H, Dorokhov V, Fast H, Gerding M, Godin-Beekmann S, Hoppel K, Johnson B, Kyro E, Litynska Z, Moore D, Nakane H, Parrondo MC, Risle AD, Skrivankova P, Stubi R, Viatte P, Yushkov V, Zerefos C. 2006. Arctic winter 2005: Implications for stratospheric ozone loss and climate change. *Geophys. Res. Lett.* **33**: L23808. doi:10.1029/2006GL026731.
- Riishojgaard LP. 1996. On four-dimensional variational assimilation of ozone data in weather prediction models. *Q. J. R. Meteorol. Soc.* **122**: 1545–1571.
- Schoeberl MR, Douglass AR, Zhu ZX, Pawson S. 2003. A comparison of the lower stratospheric age spectra derived from a general circulation model and two data assimilation systems. *J. Geophys. Res.* **108**: 4113. doi:10.1029/2002JD002652.
- Smit HGJ, Strater W, Helten M, Kley D, Ciupa D, Claude HJ, Kohler U, Hoegger B, Levrat G, Johnson B, Oltmans SJ, Kerr JB, Tarasick DW, Davies J, Shitamichi M, Srivastav SK, Vialle C, Velghe G. 1998. JOSIE: The 1996 WMO International intercomparison of ozonesondes under quasi flight conditions in the environmental simulation chamber at Jülich. In: *Proceedings of the XVIII Quadrennial Ozone Symposium*, September 1996, L'Aquila, Italy, Bojkov R, Visconti G (eds). pp. 971–974.
- Stajner I, Riishojgaard LP, Rood RB. 2001. The GEOS ozone data assimilation system: Specification of error statistics. *Q. J. R. Meteorol. Soc.* **127**: 1069–1094.
- Struthers H, Brugge R, Lahoz WA, O'Neill A, Swinbank R. 2002. Assimilation of ozone profiles and total column measurements into a global general circulation model. *J. Geophys. Res.* **107**: 4438.
- Swinbank R, Keil M, Jackson DR, Scaife AA. 2004. 'Stratospheric data assimilation at the Met Office – progress and plans'. In: *ECMWF Workshop on Modelling and Assimilation for the Stratosphere and Tropopause*, 23–26 June 2003. pp 147–154.
- Thompson AM, Witte JC, MCPeters RD, Oltmans SJ, Schmidlin FJ, Logan JA, Fujiwara M, Kirchhoff VWJH, Posny F, Coetzee GJR, Hoegger B, Kawakami S, Ogawa T, Johnson BJ, Vomel H, Labow G. 2003. Southern Hemisphere Additional Ozonesondes (SHADOZ) 1998–2000 tropical ozone climatology – 1. Comparison with Total Ozone Mapping Spectrometer (TOMS) and ground-based measurements. *J. Geophys. Res.* **108**: 8238. doi:10.1029/2001JD000967.
- Von Hobe M, Ulanovsky A, Volk CM, Grooss J-U, Tilmes S, Konopka P, Günther G, Werner A, Spelten N, Shur G, Yushkov V, Ravegnani F, Schiller C, Müller R, Stroh F. 2006. Severe ozone depletion in the cold Arctic winter 2004–05. *Geophys. Res. Lett.* **33**: L17815. doi:10.1029/2006GL026945.
- Waters JW, Froidevaux L, Harwood RS, Jarot RF, Pickett HM, Read WG, Siegel PH, Cofield RE, Filipiak MJ, Flower DA, Holden JR, Lau GK, Livesey NJ, Manney GL, Pumphrey HC, Santee ML, Wu DL, Cuddy DT, Lay RR, Loo MS, Perun VS, Schwartz MJ, Stek PC, Thurstans RP, Boyles MA, Chandra S, Chavez MC, Chen G-S, Chudasama BV, Dodge R, Fuller RA, Girard MA, Jiang JH, Jiang Y, Knosp BW, LaBelle RC, Lee KA, Miller D, Oswald JE, Patel NC, Pukala DM, Quintero O, Scaff DM, Snyder WV, Tope MC, Wagner PA, Walch MJ. 2006. The Earth Observing System Microwave Limb Sounder (EOS MLS) on the Aura satellite. *IEEE Trans. Geosci. Remote Sensing* **44**: 1075–1092.
- Žagar N. 2004. Assimilation of equatorial waves by line-of-sight wind observations. *J. Atmos. Sci.* **61**: 1877–1893.